Statistical γ decay in radiative neutron capture on rare-earth nuclei

Mgr. Stanislav Valenta, Ph.D.

April 26, 2019

After discovery of neutron by James Chadwick in 1932 the questions arrised about its interaction with matter. Two years later Enrico Fermi and colleagues observed (n,α), (n,p) and (n,γ) reactions, followed by first measurements of "surprisingly large values" of nuclear cross section for the "activating impact" of a *slow* neutron for boron, yttrium and cadmium. The neutrons were slowed down by passing through paraffin. From the experimental point of view, only one, but the crucial, piece of *the puzzle* was missing. The puzzle of harvesting the nuclear energy.

In 1936 in Nature and 1937 in Science, Niels Bohr formulated, illustrated on mechanical model and compared – to then available experimental data – his idea of compound nuclear reactions. According to Bohr the first step of the reaction is the relatively long formation of compound nucleus – the excess energy (the neutron separation energy S_n and the kinetic energy of the incident neutron) "must in this state be assumed to be temporarily stored in some complicated motions of all the particles in the compound system, and its possible subsequent breaking up with the release of some elementary or complex nuclear particle may from this point of view be regarded as a separate event not directly connected with the first stage of the collision process."

Bohr also pointed out the essential difference between the number of nuclear levels, i.e. the level density ρ, at low excitation energies (known experimentally from γ spectra after α decay), excitation energies just above neutron separation energy (known from very selective excitations by slow neutrons) and by a few MeVs higher excitation energies (indicated from fast neutron reactions), see Fig. 1. How rapidly the level density increases with excitation was at that time calculated by Bethe.

This theoretical progress was followed by the discovery of nuclear fission. In 1938, Hahn and Strassmann repeated Fermi's experiment of bombarding uranium by neutrons. Thanks to Hahn's chemical

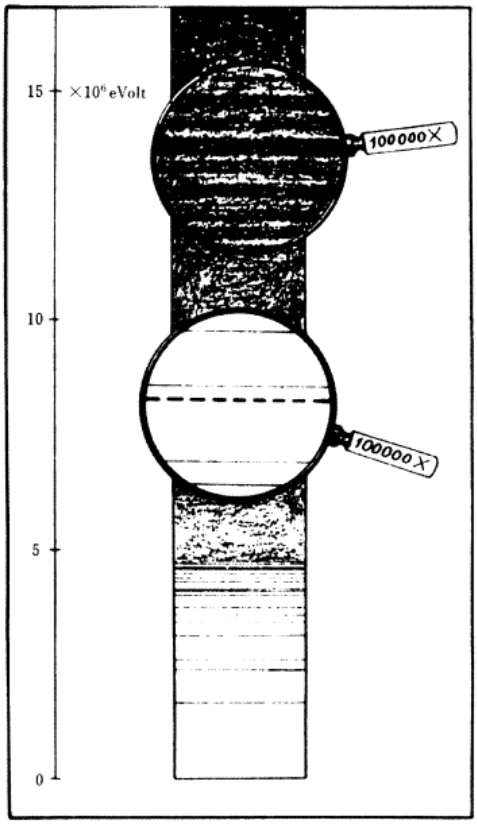

Figure 1: Bohr's illustration of "the general character of the distribution of energy levels for a heavy nucleus". The dashed line in the lower magnifying glass represents the neutron separation energy. The figure is taken from Ref. [1].

expertise, Meitner and Frisch were able to correctly interpret the production of barium in said reaction. No matter if Bohr's formulation "complex nuclear particle" accounted for fission fragments with roughly half of the uranium mass, his idea of compound nuclear reaction held for the fission reaction as well. The discovery prompted both experimental and theoretical effort. By the 1942 it was obvious that the isotope undergoing fission is ^{235}U, that the amount of released energy is significant and at least couple of neutrons are produced as well. The puzzle was complete. In December 1942, the experiment with first human-made nuclear reactor,

Chicago Pile-1, demonstrated the feasibility of controlled nuclear chain reaction.

At the end of 1950's the first commercial nuclear power plants were built. The nuclear energy became a relevant electricity source in 1970's, see Fig. 2. Since then the electricity generation increased by a factor of four with nuclear power representing about tenth.

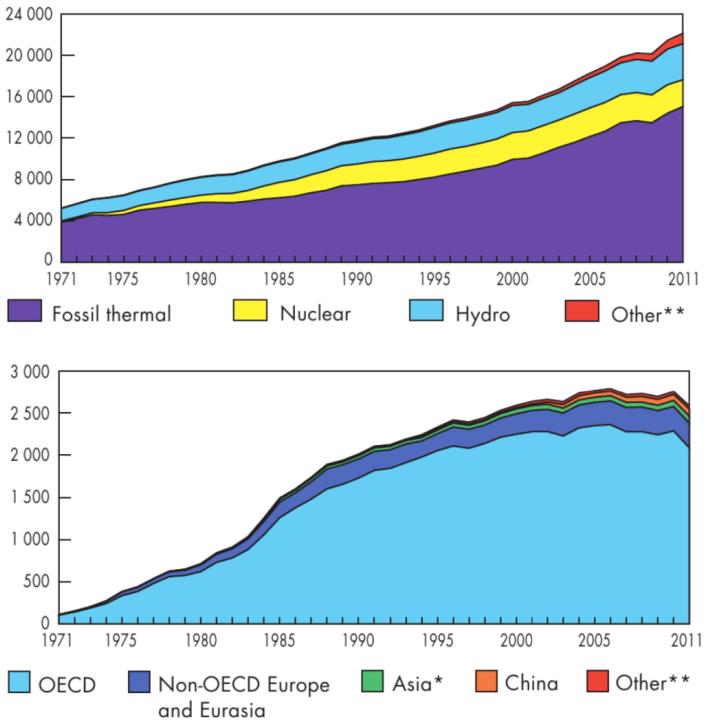

Figure 2: (Top) World electricity generation from 1971 to 2011 by fuel (TWh). (**) Other includes geothermal, solar, wind, biofuels and waste, and heat. (Bottom) Nuclear production from 1971 to 2011 by region (TWh). (*) Asia excludes China. (**) Other includes Africa, Non-OECD Americas and the Middle East. The figures are taken from Ref. [2].

Natural uranium contains more than 99% of ^{238}U and less than 1% of ^{235}U, which is fissile with thermal neutron (a free neutron with a kinetic energy of about 0.025 eV). While some nuclear reactors can run with natural uranium, vast majority of present nuclear reactors in powerplants operate with low-enriched uranium fuel exploiting the fissile isotope ^{235}U. After enrichement the fuel still contains more than 80% of ^{238}U. The neutron-induced reactions on this isotope (and the reactions competing with fission on ^{235}U) give raise to isotopes of transuranium elements such as plutonium and americium. The total radiotoxicity of nuclear waste becomes dominated by these transuranium actinides after few tens of years and does not fall to the level of natural uranium even after milion years [3]. Apart from a possibility of long term storage of the nuclear waste, there are concepts for it transmutation using faster neutrons, e.g. integral fast reactor or accelerator-driven system.

In line with the above, the need to measure the neutron-induced reactions on actinides is evident, which is clearly reflected by the community, see the Nuclear Data High Priority Request List in Fig. 3. For epithermal and higher neutron energies, the cross section (as a function of neutron energy) of the ^{235}U(n,γ) reaction is requested to be measured with better than 3% uncertainty; ^{238}U(n,γ) with $\sim$ 2% uncertainty.

The (n,γ) reaction, i.e. the radiative neutron capture, is depicted in Fig. 4. A neutron is captured on target nucleus (with A nucleons) resulting in compound, $A+1$ nucleus. The compound is in excited state with energy given by the sum of neutron separation energy B_n of compound nucleus and the kinetic energy of incoming neutron. If this excitation energy coincides with excitation energy of nuclear level, a significant increase in cross section, a neutron resonance, is observed. There are few isotopes for which such increase is observed with thermal neutrons. Because of that, gadolinium, a rare-earth element, is used as burnable neutron absorber in fresh uranium fuel. Sensitivity and uncertainty analyses show that keeping the ^{155,157}Gd(n,γ) cross sections uncertainties below 4% mitigates the impact on reactivity uncertainty at high-burnup, which is important for a good estimation of the residual reactivity penalty of a fuel assembly at the end of life [4].

The excited state of compound nucleus deexcites by emitting a cascade of γ rays. The typical neutron separation energies for rare-earths and actinides are $B_n \approx 5-7$ MeV and there are typically milions of nuclear levels between ground state and neutron resonances.

The decay of levels at low excitation energies, at most a few of MeV, is known experimentally. The properties of low-lying levels are predicted in theoretical models. The collective effects such as vibrations and rotations often play crucial role in the character of these levels and hence implicate their decay probabilities.

From certain excitation energy experiment can not resolve levels anymore and the theoretical calculations become extremely difficult. As the goal is to describe the radiative decay of highly excited levels, e.g. neutron resonances, one has to use other approach – the statistical model of γ decay suppresses the individuality of nuclear levels and sta-

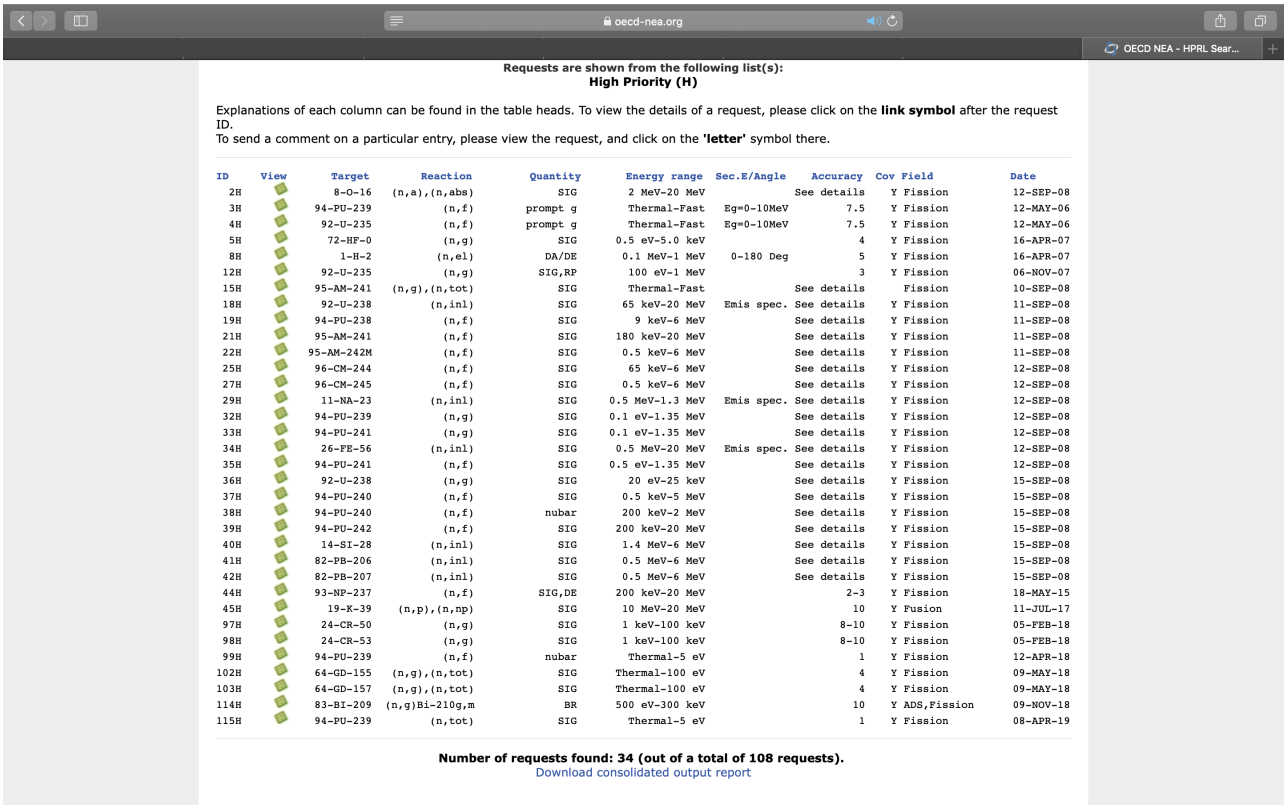

oecd-nea.org

OECD NEA - HPRL Sear...

Requests are shown from the following list(s):
High Priority (H)

Explanations of each column can be found in the table heads. To view the details of a request, please click on the **link symbol** after the request ID.
To send a comment on a particular entry, please view the request, and click on the **'letter'** symbol there.

ID	View	Target	Reaction	Quantity	Energy range	Sec.E/Angle	Accuracy	Cov	Field	Date
2H		8-O-16	(n,a),(n,abs)	SIG	2 MeV-20 MeV		See details	Y	Fission	12-SEP-08
3H		94-PU-239	(n,f)	prompt g	Thermal-Fast	Eg=0-10MeV	7.5	Y	Fission	12-MAY-06
4H		92-U-235	(n,f)	prompt g	Thermal-Fast	Eg=0-10MeV	7.5	Y	Fission	12-MAY-06
5H		72-HF-0	(n,g)	SIG	0.5 eV-5.0 keV		4	Y	Fission	16-APR-07
8H		1-H-2	(n,el)	DA/DE	0.1 MeV-1 MeV	0-180 Deg	5	Y	Fission	16-APR-07
12H		92-U-235	(n,g)	SIG,RP	100 eV-1 MeV		3	Y	Fission	06-NOV-07
15H		95-AM-241	(n,g),(n,tot)	SIG	Thermal-Fast		See details		Fission	10-SEP-08
18H		92-U-238	(n,inl)	SIG	65 keV-20 MeV	Emis spec.	See details	Y	Fission	11-SEP-08
19H		94-PU-238	(n,f)	SIG	9 keV-6 MeV		See details	Y	Fission	11-SEP-08
21H		95-AM-241	(n,f)	SIG	180 keV-20 MeV		See details	Y	Fission	11-SEP-08
22H		95-AM-242M	(n,f)	SIG	0.5 keV-6 MeV		See details	Y	Fission	11-SEP-08
25H		96-CM-244	(n,f)	SIG	65 keV-6 MeV		See details	Y	Fission	12-SEP-08
27H		96-CM-245	(n,f)	SIG	0.5 keV-6 MeV		See details	Y	Fission	12-SEP-08
29H		11-NA-23	(n,inl)	SIG	0.5 MeV-1.3 MeV	Emis spec.	See details	Y	Fission	12-SEP-08
32H		94-PU-239	(n,g)	SIG	0.1 eV-1.35 MeV		See details	Y	Fission	12-SEP-08
33H		94-PU-241	(n,g)	SIG	0.1 eV-1.35 MeV		See details	Y	Fission	12-SEP-08
34H		26-FE-56	(n,inl)	SIG	0.5 MeV-20 MeV	Emis spec.	See details	Y	Fission	12-SEP-08
35H		94-PU-241	(n,f)	SIG	0.5 eV-1.35 MeV		See details	Y	Fission	12-SEP-08
36H		92-U-238	(n,g)	SIG	20 eV-25 keV		See details	Y	Fission	15-SEP-08
37H		94-PU-240	(n,f)	SIG	0.5 keV-5 MeV		See details	Y	Fission	15-SEP-08
38H		94-PU-240	(n,f)	nubar	200 keV-2 MeV		See details	Y	Fission	15-SEP-08
39H		94-PU-242	(n,f)	SIG	200 keV-20 MeV		See details	Y	Fission	15-SEP-08
40H		14-SI-28	(n,inl)	SIG	1.4 MeV-6 MeV		See details	Y	Fission	15-SEP-08
41H		82-PB-206	(n,inl)	SIG	0.5 MeV-6 MeV		See details	Y	Fission	15-SEP-08
42H		82-PB-207	(n,inl)	SIG	0.5 MeV-6 MeV		See details	Y	Fission	15-SEP-08
44H		93-NP-237	(n,f)	SIG,DE	200 keV-20 MeV		2-3	Y	Fission	18-MAY-15
45H		19-K-39	(n,p),(n,np)	SIG	10 MeV-20 MeV		10	Y	Fusion	11-JUL-17
97H		24-CR-50	(n,g)	SIG	1 keV-100 keV		8-10	Y	Fission	05-FEB-18
98H		24-CR-53	(n,g)	SIG	1 keV-100 keV		8-10	Y	Fission	05-FEB-18
99H		94-PU-239	(n,f)	nubar	Thermal-5 eV		1	Y	Fission	12-APR-18
102H		64-GD-155	(n,g),(n,tot)	SIG	Thermal-100 eV		4	Y	Fission	09-MAY-18
103H		64-GD-157	(n,g),(n,tot)	SIG	Thermal-100 eV		4	Y	Fission	09-MAY-18
114H		83-BI-209	(n,g)Bi-210g,m	BR	500 eV-300 keV		10	Y	ADS,Fission	09-NOV-18
115H		94-PU-239	(n,tot)	SIG	Thermal-5 eV		1	Y	Fission	08-APR-19

Number of requests found: 34 (out of a total of 108 requests).
Download consolidated output report

Figure 3: NEA Nuclear Data High Priority Request List [4].

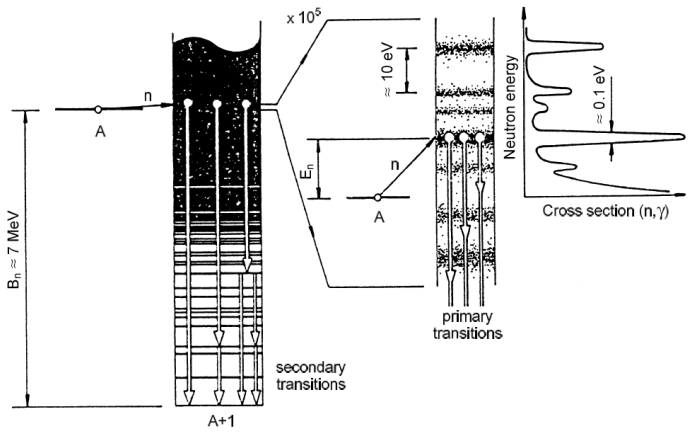

Figure 4: Schema of radiative neutron capture reaction.

tistically investigates their behavior. The decay is then described using average quantities, namely level density and photon/radiative/γ-ray strength functions (PSFs), and fluctuation properties, that is the counting uncertainty and correlations in level density and the so-called Porter-Thomas fluctuations of partial radiation widths (the probabilities of decay from one level to all other accessible ones).

When measuring the cross section of neutron-induced reactions, the products of the reactions are in fact measured. Hence, in order to achieve the above mentioned requested precisions, the process of γ deexcitation of compound nuclei of interest should be understood as best as possible. The current knowledge of cross sections for ^{235}U and ^{163}Dy is shown in Fig. 5. The radiative neutron capture dominates over other possible reactions in the case of rare-earth nuclei, while in actinides one often deals with fissile targets. During fission γ rays are emitted as well, which is one of the factors making the measurements of (n,γ) cross section rather challenging.

Luckily, the actinides and rare-earths display some key similarities – the isotopes are deformed, see Fig. 6, and they exhibit high level density as mentioned above. This enables us to use the analysis processes and the knowledge of photon strength functions in rare-earths when dealing with experimentally more complicated cases of actinides.

From the fundamental point of view, the so-called Scissors Mode was predicted in deformed nuclei by theory (in Interacting Boson Model [7, 8] and Two-Rotor Model [9]). The out-of-phase oscillations of neutron and proton fluids as illustrated in Fig. 7 give raise to a concentration of $M1$ collective states at excitation energy of about 3 MeV. The mode was discovered in (e,e′) experiment on ^{156}Gd [10] and soon after measured in ^{164}Dy with transition strength $1.5(3)\mu_N^2$ [11]. A systematic study of the mode for the ground-state transitions in rare-earth nuclei was performed with help of the (γ,γ') reaction – the so-called nuclear resonance fluorescence scattering (NRF) experiments [12]. The strength of

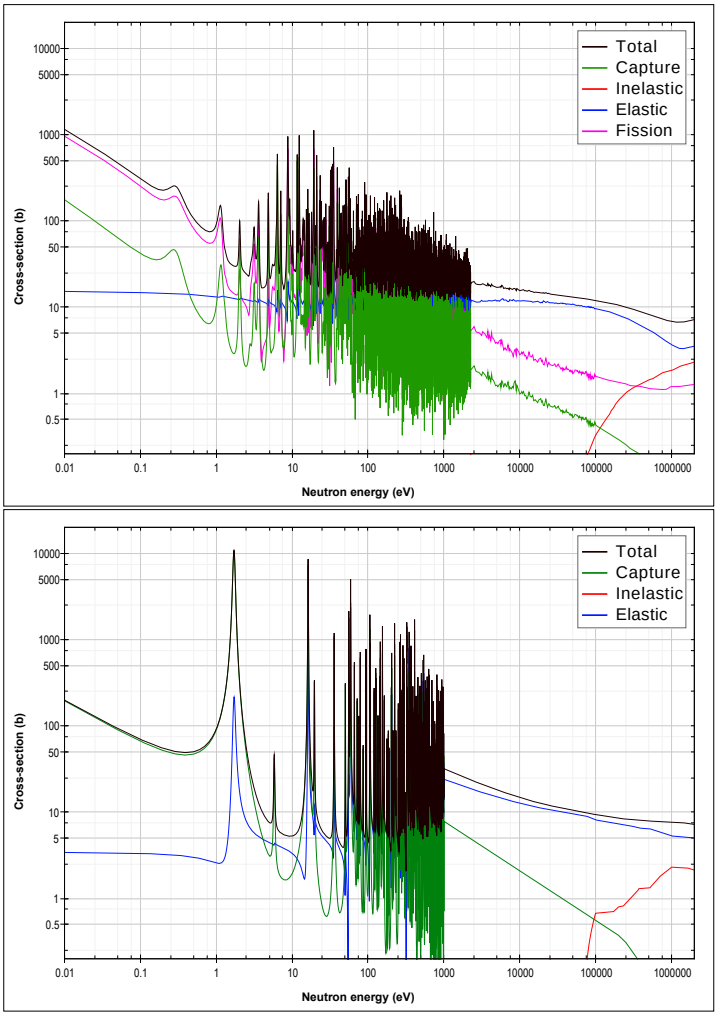

Figure 5: Total and partial cross sections of neutron induced reactions for ^{235}U (left) and ^{163}Dy (right). The data are taken from ENDF/B-VII.0 database [5].

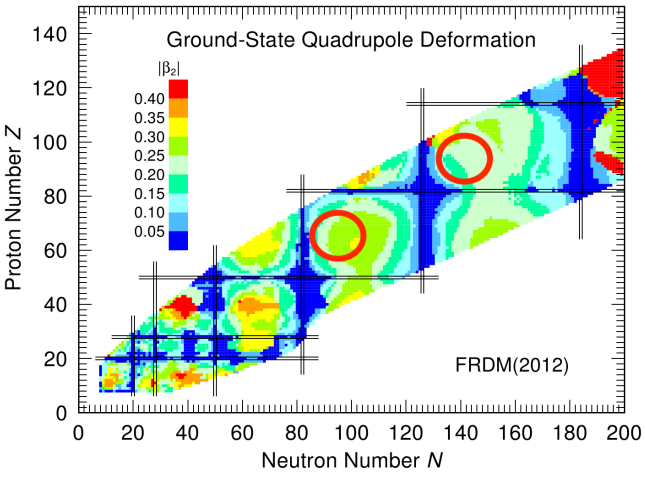

Figure 6: Ground-state quadrupole deformations of nuclei as calculated in Ref. [6]. The rare-earth and actinide nuclei, marked by red circles, exhibit very similar deformations.

the mode was found to be close to $3\mu_N^2$ in even-even well-deformed rare-earth nuclei.

The role of the scissors mode in deexcitation of

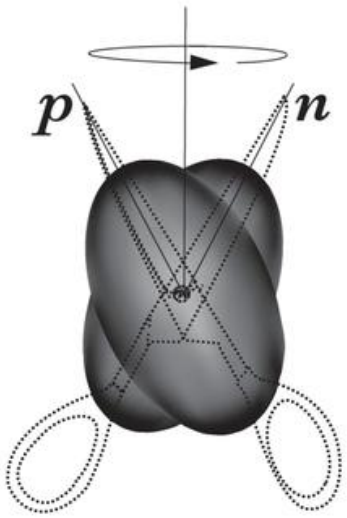

Figure 7: The interpretation of scissors mode.

nuclear levels was examined mainly in radiative neutron capture and ^{3}He-induced reactions in Oslo Cyclotron Laboratory. Data on two-step γ cascades (TSCs), measured by a pair of HPGe detectors at research reactor LVR-15 in Řež, following the thermal neutron capture on ^{162}Dy nucleus revealed that enhancement of $M1$ transitions by SM in radiative decay is more general property influencing even nuclear levels with excitation energy of several MeV [13, 14]. The scissors mode was represented by Lorentzian term in $M1$ PSF centered at 3 MeV with integrated strength of $6.2\mu_N^2$ [14]. The Oslo results on SM parameters of ^{163}Dy were consistent with those coming from TSC data, authors reported the SM strength of $7.8(22)\mu_N^2$ [15].

Futhermore, the strength of SM derived by the Oslo method in neighboring even-even dysprosium isotopes was claimed to be comparable to SM strength in ^{163}Dy, e.g. $6.8(8)\mu_n^2$ in ^{162}Dy [16].

Within the scope of PhD studies of J. Kroll (started 2009) and S. Valenta (2010) under supervision of M. Krtička and F. Bečář several multi-step γ cascades (MSC) and TSC experiments were analysed. The MSCs were measured by the DANCE detector array at Los Alamos Neutron Science Center in Los Alamos National Laboratory.

Contrary to the Oslo result, the systematic study of SM in gadolinium isotope chain using the abovementioned data on MSC accompanying the resonance neutron capture [17, 18, 19] revealed that the strength of the mode in even-even nuclei is 2–3 times lower compared to neighboring odd ones, e.g. $2.7(8)\mu_N^2$ and $8.0(1.5)\mu_N^2$ in ^{156}Gd and ^{157}Gd respectively.

The main result of the TSC analysis [20] of ^{155,157}Gd(n,γ) reaction regarding the PSFs is that

the TSC spectra are reproduced by the PSFs determined in the MSC analyses [17, 18].

The analysis of MSC from resonance neutron capture on dysprosium isotopes published in [21, 22] yielded: (i) results consistent with TSC ones [13, 14] for ^{163}Dy, (ii) similar, albeit not as pronounced trend between even-even and odd isotopes as in case of gadolinium analyses [17, 18, 19] and (iii) for the first time a hint that the statistical model prescription for the fluctuations of partial radiative widths might be inadequate. The main results on the scissors mode parameters are given in Tab. 1.

	Scissors mode parameter		
Isotope	centroid (MeV)	width (MeV)	strength (μ_N^2)
^{162}Dy	2.8 - 3.0	1.0 - 1.4	2.3 - 4.3
^{163}Dy	3.0 - 3.1	0.8 - 1.2	5.4 - 9.0
^{164}Dy	2.8 - 3.0	1.0 - 1.4	5.3 - 7.5

Table 1: Scissors mode parameters reproducing the average MSC spectra of dysprosium isotopes.

The overall consistency of results from thermal (TSC) and resonance (MSC) neutron capture is encouraging, the description of γ decay was proven adequate in recently published measurement of (n,γ) cross section using liquid scintillation detectors at the neutron time-of-flight facility n_TOF at CERN [23]. On the other hand, one has to keep in mind that there are significant differences to Oslo results that need to be addressed.

First results on PSFs in actinides have been published by the Oslo group [24] and from the measurements with DANCE [25]. Both groups of authors have benefited from the experience with analysis of rare-earth nuclei. The ongoing analyses of MSC spectra and cross sections of radiative neutron capture on ^{233,234,238}U measured at n_TOF are benefiting from the same expertise as well.

References

[1] N. Bohr, Science **86** (1937) 161.

[2] International Energy Agency, *Key World Energy Statistics 2013*, 2013.

[3] IAEA, *Classification of radioactive waste: safety guide*, 2009.

[4] Nuclear Energy Agency, *NEA Nuclear Data High Priority Request List*, 2019. as available at https://www.oecd-nea.org/dbdata/hprl/.

[5] D. Brown, M. Chadwick, R. Capote, *et al.*, Nuclear Data Sheets **148** (2018) 1 – 142, Special Issue on Nuclear Reaction Data.

[6] P. Möller, A. Sierk, T. Ichikawa, and H. Sagawa, Atomic Data and Nuclear Data Tables **109-110** (2016) 1 – 204.

[7] R. R. Hilton, Proc. of the International Conference on Nuclear Structure in Dubna (1976), unpublished.

[8] N. L. Iudice and F. Palumbo, Phys. Rev. Lett. **41** (1978) 1532.

[9] F. Iachello, Nucl. Phys. A **358** (1981) 89c.

[10] D. Bohle *et al.*, Phys. Lett. B **137** (1984) 27.

[11] D. Bohle *et al.*, Phys. Lett. B **148** (1984) 260.

[12] U. Kneissl, H. H. Pitz, and A. Zilges, Prog. Part. Nucl. Phys. **37** (1996) 349.

[13] F. Bečvář *et al.*, Phys. Rev. C **52** (1995) 1278.

[14] M. Krtička *et al.*, Phys. Rev. Lett. **92** (2004) 172501.

[15] H. T. Nyhus *et al.*, Phys. Rev. C **81** (2010) 024325.

[16] M. Guttormsen *et al.*, Phys. Rev. C **68** (2003) 064306.

[17] A. Chyzh *et al.*, Phys. Rev. C **84** (2011) 014306.

[18] B. Baramsai *et al.*, Phys. Rev. C **87** (2013) 044609.

[19] J. Kroll *et al.*, Phys. Rev. C **88** (2013) 034317.

[20] S. Valenta *et al.*, Phys. Rev. C **92** (2015) 064321.

[21] S. Valenta *et al.*, Phys. Rev. C **96** (2017) 054315.

[22] S. Valenta, *Study of statistical γ decay in well-deformed rare-earth nuclei*. PhD thesis, Charles University, 2018.

[23] n_TOF Collaboration, M. Mastromarco *et al.*, Eur. Phys. J. A **55** (2019) 9.

[24] M. Guttormsen *et al.*, Phys. Rev. C **89** (2014) 014302.

[25] J. L. Ullmann *et al.*, Phys. Rev. C **96** (2017) 024627.